Optics Communications 501 (2021) 127362

Contents lists available at ScienceDirect

Optics Communications

journal homepage: www.elsevier.com/locate/optcom

Waveguide shape and waveguide core size optimization of Y-branch optical splitters up to 128 splitting ratio

Stanislava Serecunova [a,b], Dana Seyringer [c,*], Frantisek Uherek [d,b], Heinz Seyringer [a]

[a] V-Research GmbH, Stadtstraße 33, 6850 Dornbirn, Austria
[b] Institute of Electronics and Photonics, FEI STU, Ilkovicova 3, 812 19 Bratislava, Slovakia
[c] Research Centre for Microtechnology, Vorarlberg University of Applied Sciences (FHV), Hochschulstraße 1, 6850 Dornbirn, Austria
[d] International Laser Centre, Ilkovicova 3, 841 04 Bratislava, Slovakia

ARTICLE INFO

Keywords:
Y-branch splitter
S-Bend
Light propagation
Telecommunications

ABSTRACT

In this paper, low-loss Y-branch splitters up to 128 splitting ratio are designed, simulated, and optimized by using 2D beam propagation method in OptiBPM tool by Optiwave. For an optical waveguide, a silica-on-silicon material platform is used. The splitters were designed as a planar structure for a telecommunication operating wavelength of 1.55 μm. According to the minimum insertion loss and minimum non-uniformity, the optimum length for each Y-branch is determined. The influence of the pre-defined S-Bend waveguide shapes (Arc, Cosine, Sine) and of the waveguide core size reduction on the splitter performance has been also studied. The obtained simulation results of all designed splitters with different S-Bend shape waveguides together with the different waveguide core sizes are discussed and compared with each other.

1. Introduction

Optical fibers are by far the most promising means of transmission for a rapidly growing need of higher data frequency, and broadband services in the telecommunication market. One of the most effective technologies in development of fiber optic access is the passive optical network (PON) [1]. Thus, an optical distribution infrastructure consists only of passive optical components such as optical fibers, connectors, and optical splitters. They require no power, no climate control, and no maintenance whatsoever. Their advantage is that they will keep working until they are physically impacted. In the past decade, PON architectures are being developed and standardized by ITU-T and IEEE [2].

The PON offers extensive advantages when deployed the Fiber-To-The-x (FTTx) architecture. Telecom operators generally use this technology to enable high-bandwidth terminal internet services and apply EPON / GPON / 10G-EPON simultaneously for multiple users at the same time at home (FTTH), building (FTTB), premises (FTTP), or other locations, depending on where the optical fiber is terminated. The main application of PON is Fiber-To-The-Home (FTTH). The signal carried on a feeder fiber can be split to provide service with an optical line terminal (OLT) to serve multiple premises up to 128 users with an Optical Network Unit (ONU) or Optical Network Terminal (ONT) converting the signals and providing users with internet access in the form of point to multipoint (P2MP) architecture [3,4].

Splitting and combining of multiple optical beams plays an important role in photonic technologies [5,6]. A passive optical splitter is a planar waveguide structure that divides the light beam, coupled into the input port, in two or multiple separate light beams on the output ports. The same approach can be used in the reverse direction to combine multiple optical light beams, coupled at the output ports, into one input port as well [7].

There are two main approaches used to split one input optical signal into N output signals. The most apparent way is to use a series of one-by-two waveguide branches in a cascade (also called Y-branches) [8]. In this approach ideally half of the input beam power goes to the first branch and the other half to the second branch [9]. However, the processing of the branching point, where two waveguides start to separate, is technologically very difficult [10] which generally leads to an asymmetric splitting ratio causing non-uniformity of the split power over all the output waveguides. On the other hand, these splitters have two significant advantages, namely they are polarization and wavelength independent, i.e., one device can be used to split optical signals in the whole telecommunication operating wavelength window.

In contrast to the Y-branch approach, the multimode interference (MMI) splitters are based on splitting the optical signal on the self-imaging effect — a property of existed modes, which reproduces the input field profile in one or more images at regular intervals along the direction of waveguide propagation. This is due to constructive interference between higher modes (superposition of modes with different propagation speeds), which appears inside the multimode section.

* Corresponding author.
E-mail address: dana.seyringer@fhv.at (D. Seyringer).

https://doi.org/10.1016/j.optcom.2021.127362
Received 14 June 2021; Received in revised form 28 July 2021; Accepted 10 August 2021
Available online 17 August 2021

By cutting the MMI coupler at a particular length, N output signals can be obtained. The MMI splitters feature a large splitting number and stable splitting ratio, ensuring good uniformity over all the output signals. Furthermore, the MMI splitters are potentially shorter in comparison to Y-branching-type splitters [11]. Another advantage is their good fabrication tolerance because the splitting is performed in the multimode section. Their main disadvantage results from the fact that the length of the multimode section is wavelength dependent, i.e., the MMI splitters are designed solely for one wavelength and can only operate in a narrow wavelength band. They are also polarization dependent; however, it has been shown that for strong guidance waveguide structures, this dependency has been proven to be minimal [12,13]. The MMI splitters are also widely used in various optical devices, including power, wavelength, and polarization splitters, switches, and add–drop multiplexers.

The performance characteristics of the splitters depend largely on the optical properties of the waveguide materials used. They can be fabricated on various material platforms such as silica-on-silicon (SoS) buried waveguides [14], silicon-on-insulator (SOI) ridge waveguides [15–17], SOI-nanowires [18], buried InP/InGaAsP ridge waveguides [19], polymer waveguides [20,21], or Si_3N_4 waveguides [22]. SoS-based waveguide devices use for the most part SiO_2-buried rectangular waveguides, usually with a cross-section of (6 × 6) μm^2 and a low refractive-index contrast between the core (waveguide) and the cladding, $\Delta n \sim 0.011$ (this parameter is also often expressed in percent as $\Delta n \sim 0.75\%$, from $(n_c - n_{cl})\cdot 100/n_c$) [23]. Low-index-contrast waveguide devices still hold a large share of the market because of their many advantages. First, their modal field matches well with that of single-mode optical fibers, making it relatively easy to couple them to fibers. Second, they combine low propagation loss (<0.05 dB/cm, because there is little absorption and scattering in the waveguides) with a high fiber-coupling efficiency (low losses on the order of 0.1 dB) [24]. However, the very low refractive-index contrast means the bending radius of the waveguides needs to be very large (on the order of several millimeters) and may not fall below a particular, critical value to suppress bending losses. As a result, silica-based waveguide devices usually have a very large size that limits the integration density of SiO_2-based photonic integrated devices.

High-index-contrast splitters, such as SOI-based waveguide devices, use a high refractive-index difference $\Delta n \sim 2.055$ for Si/SiO_2 (~2.5 for Si/air) between the refractive indices of the core (Si, $n_c \sim 3.5$) and the cladding (Si_2, $n_{cl} \sim 1.445$, or air, $n_{cl} = 1.0$) [23] (in percent, $\Delta n \sim 58\%$). This is approximately 100 times higher than that of typical SoS waveguides. Due to the fact that a waveguide's size decreases proportionally to the increase in refractive index contrast, the waveguide size for this material composition shrinks into the nanometer scale. Such high-index contrast makes it possible to guide light in waveguides with a far smaller bending radius (bending on the scale of several tens of microns), which leads to a significant reduction in the size of the structure by more than two orders of magnitude when compared to devices based on silica materials [25–27]. Such compact devices can easily be implemented on-chip. The main problem arising from the reduced size of waveguides is the coupling of the optical signal from the fiber into such small input waveguides which causes much higher coupling losses, on the order of 10 dB, than in silica waveguide devices. In addition, in Si-nanowire waveguides, the scattering loss (per unit of length) is much larger than the loss for conventional low-index-contrast waveguides due to the light scattering on imperfections of the fabricated waveguide sidewalls [28]. In order to reduce the roughness of these sidewalls and thus minimize such high-dimensional fluctuations, the SOI-nanowire waveguide devices require very-high-resolution fabrication technology that still presents a considerable challenge today. An alternative to high-index-contrast and low-index-contrast waveguide components is the Si_3N_4 material platform, which has a moderate index contrast lying between both main groups [29].

Based on the advantages listed above, the most common splitters deployed in PON system are SoS based (low-index contrast) Y-branch optical splitters [8]. As already mentioned, their main advantages are the polarization and wavelength independence together with the significantly low propagation and coupling losses. Their drawbacks are the asymmetric splitting ratio (non-uniformity of split power), and the large size of the splitter structure. These parameters define the final performance of the splitter. The principal factors determining the size are the used material type and the length of the individual waveguide branches with a corresponding angle. By decreasing the length of the splitting branches, the angle of the waveguide is increasing, which leads to higher bending losses. By increasing the length of the Y-branches the losses decrease and saturate at a particular length. The objective is to find this length which is a final shortest possible length for each splitting Y-branch leading to a significant length reduction of the whole designed splitter. The second drawback of the Y-branch splitters is a high asymmetric splitting of the optical signal. This parameter depends on both, the design, and the fabrication process. From technological point of view, the fabrication process has only a week influence on the splitting parameter since the size of the used SoS waveguides is large in comparison to the small dimensional fluctuations caused by the fabrication. From the design point of view, it will be shown that applying the waveguide core size optimization, the high asymmetric splitting can be substantially suppressed.

The remainder of this paper is organized as follows: In Section 2, a short summary of the related work is presented. Section 3 deals with the design, simulation, and optimization, the influence of the waveguide length with different S-Bend waveguide shapes on the final performance of Y-branch optical splitters, and possible optimization by decreasing waveguide core size. Section 4 describes the mathematical analysis of the simulated results. Section 5 critically assesses achieved results. Finally, concluding remarks are presented in Section 6.

2. State of the art

Over the past years, various passive optical components for telecommunication have been developed. In this section, relevant work addressing a 1 × 128 Y-branch splitter, the splitter with the highest splitting ratio presented in this paper, is introduced. For the mathematical analysis, the beam propagation method (BPM) was used for all the below-related works.

The first design of 1 × 128 Y-branch splitter was proposed by Takahashi already in 1991 [30]. The splitter was designed with silica-based waveguides having the refractive index difference 0.75 %. Their design consists of two regions: branching and fanout. The core thickness throughout the splitter was kept constant, 5 μm. However, the core width was varying according to the region provided by tapered connections: 5.5 μm in the branching region and 7 μm in the fanout region. The port pitch between output branches was 250 μm. The maximum insertion loss of the splitter was −25.9 dB and minimum insertion loss −22.2 dB, with the non-uniformity 3.6 dB.

In 2014 Wang et al. [31] proposed a different approach of 1 × 128 Y-branch splitter, with the port pitch of 127 μm. Splitter was composed of silica waveguides with refractive index contrast of 0.45% between core and cladding, where the refractive index of the core was 1.4515 and of the cladding 1.445, respectively. The core size was (6.5 × 6.5) μm^2 and the splitter reached the size (27.7×16.7) mm^2, which was nearly half size of the optical power splitter proposed by Takahashi et al. The insertion loss was −22.8 dB and non-uniformity 1.4 dB.

KwangOk et al. [32] performed the PON extender of 10G-EPON which can support up to 80 km transmission distance at feeder section and provides split ratios of 1 × 128 on a 10 or 20 km reach at the distribution section. The 1 × 128 splitter was designed using one 1 × 4 and four 1 × 32 optical splitters which were connected to 128 ONUs. The insertion loss of the splitter was about −23 dB.

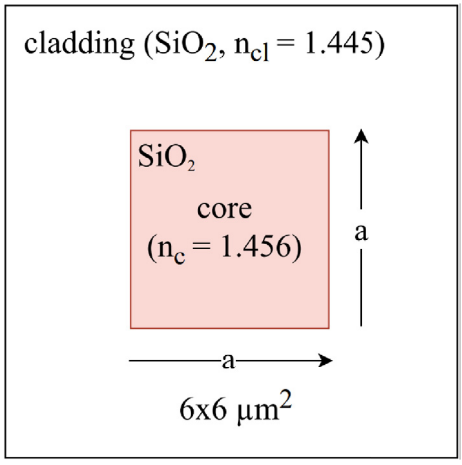

Fig. 1. The cross-section view of SoS rectangular waveguide structure.

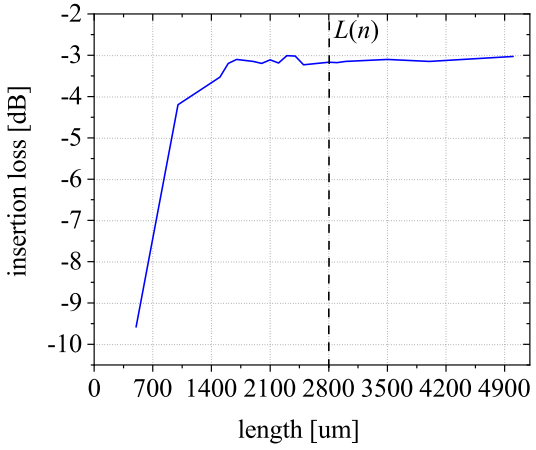

Fig. 3. Scanning of the length of the branches based on the minimum bending losses.

3. Design and simulation

The optical splitters presented here are designed and simulated at the telecommunication operating wavelength, $\lambda = 1.55$ μm. The optical waveguide structure, used in the design of all Y-branch optical splitters, is a silica-on-silicon (SoS) buried rectangular channel, as shown in Fig. 1. It consists of a core layer with a refractive index $n_c = 1.456$, which is transversely surrounded by a cladding layer having a refractive index $n_{cl} = 1.445$. The refractive-index contrast between the cladding and the core is $\Delta n = 0.75\%$. The waveguides were set to have a core size (6×6) μm^2, which is today a standard size used in passive waveguide optical components for telecommunication applications [33–35]. A guided optical wave then propagates in the waveguide along with its longitudinal direction.

3.1. Length optimization

A conventional Y-branch splitter structure consists of an input waveguide, splitting waveguides, and output waveguides, as presented in Fig. 2. The input waveguide is required to link the light beam from optical fiber into splitter and the output waveguides are used to stabilize the light beam. Both are set to have a length of $L(in) = L(out) = 500$ μm. The waveguides placed between the input/output waveguides are used for a splitting of the optical signal. To keep the whole length of the splitters L as short as possible, every Y-branch is individually scanned between selected length ranges, as shown in Fig. 3. From the graph, it is evident that the optical power is damped approximately up to 2100 μm branch length. In this length range, the angle of the waveguide is too steep causing high bending losses. By increasing the length of the Y-branches the losses decrease and saturate at a particular length $L(n)$. This length is chosen as a final shortest possible length for each Y-branch. From Fig. 3 is evident that in the case of the last branch $L(n)$, the bending loss is significantly reduced approximately at 2800 μm length. Therefore, the length of all last Y-branches $L(n)$ is set to this value. The port pitch between all output waveguides $P(n)$ was set to 127 μm. This value is required for a connection with the fibers. Each next port is then doubled in every next splitting phase between the branches in the direction to the input waveguide.

The branches with a final lengths were joined to reach a splitting ratio from 2 to 4… to 128 outputs. Fig. 4 shows the design of the final length-optimized 1×128 Y-branch splitter with Arc S-Bend waveguide shape.

3.2. Waveguide shape optimization

Fig. 5 shows the geometry of the pre-defined S-Bend Arc shape waveguide used in the splitter design presented in Fig. 4. The splitting

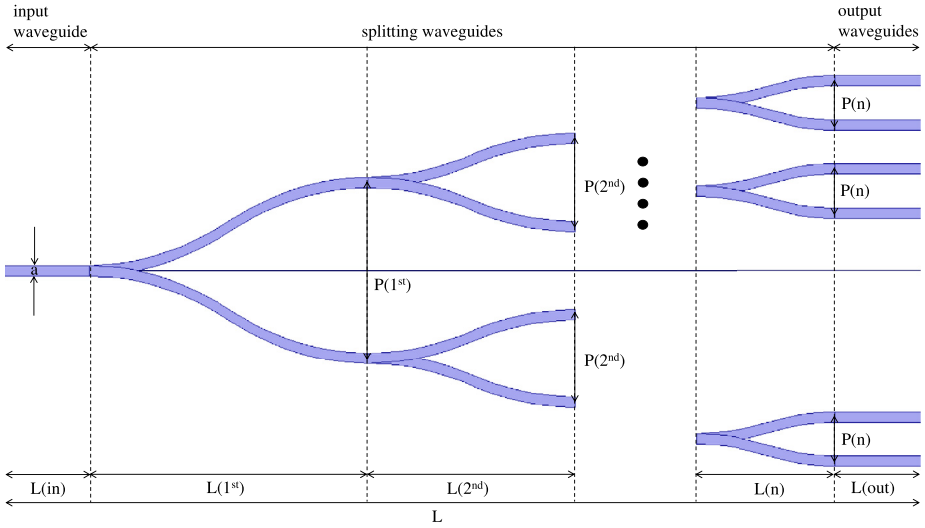

Fig. 2. Schematic view of the proposed 1×128 Y-branch splitter.

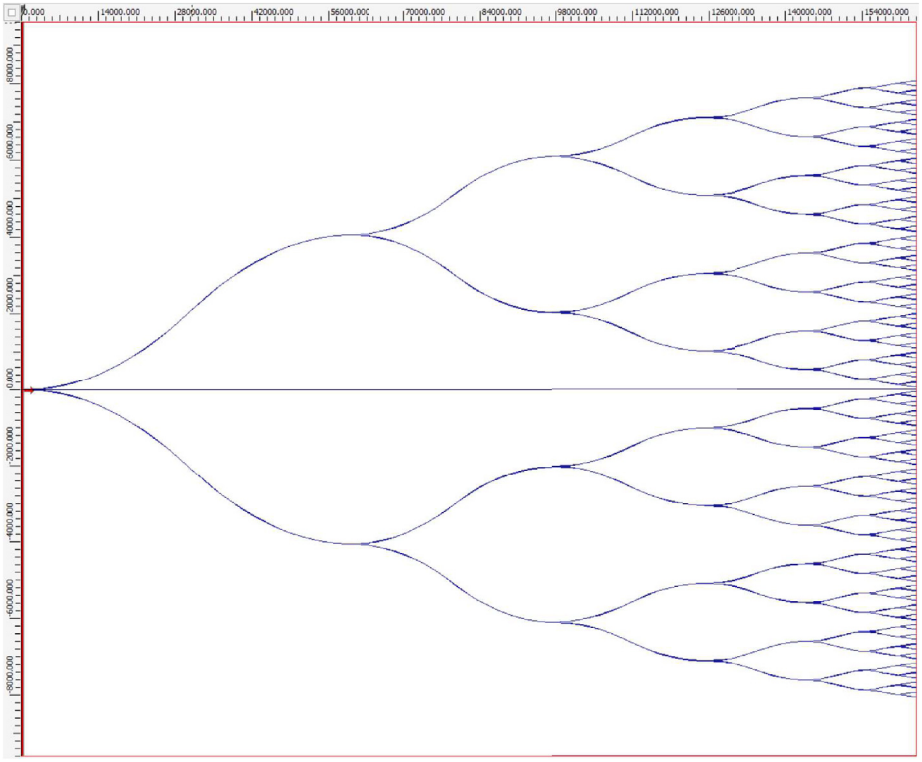

Fig. 4. Design of 1 × 128 Y-branch optical splitter with Arc S-Bend waveguides shape.

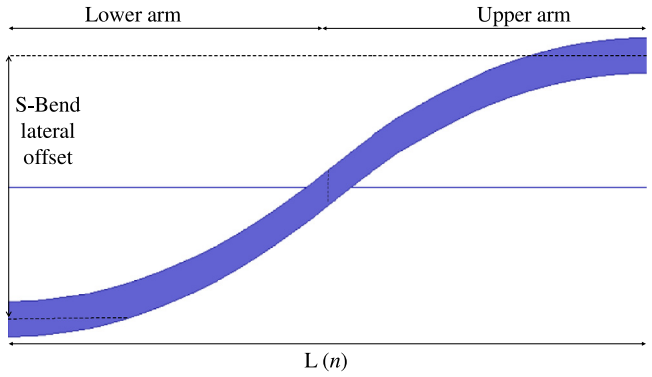

Fig. 5. S-Bend Arc waveguide.

Table 1
Summary of lengths of Y-branches in the 1 × 128 splitter with different waveguide shapes and waveguide core size (6 × 6) μm^2.

Length of Y-branch [μm]	Waveguide shape		
	Arc	Cosine	Sine
L(1st)	59500	59500	26500
L(2nd)	37000	39000	21500
L(3rd)	28000	29000	20500
L(4th)	18500	20500	13500
L(5th)	10500	9500	10500
L(6th)	6000	6500	6500
L(7th)	2800	2700	2600

waveguides use mainly S-Bend shapes because these provide low-loss between waveguides with S-Bend lateral offset. There are basically three pre-defined types of S-Bend waveguide shapes in OptiBPM layout. These are Arc, Sine, and Cosine. They can be defined in terms of their path, or by specifying the upper and lower arms of the waveguide, as shown in Fig. 5 [36]. In our designs the S-Bend lateral offset of the arms was set to 63.5 μm to ensure the coupling of the light to single mode fibers. From this follows that the last Y-branches will have port pitch 2×63.5 = 127 μm. Radius of the S-Bend was calculated automatically by the tool based on the length and lateral offset of the S-Bend waveguide.

To study the influence of the various shapes on the splitter performance, the length of the splitter was optimized for all S-Bend shapes provided by OptiBPM tool. After scanning the lengths $L(n)$ of all Y-branches for all particular port pitches $P(n)$ with all S-Bend shapes (shown in Table 1) the Y-branches were joined together to create the final 1×2^N splitters. For instance, the 1 × 4 Y-branch splitter structure contains one Y-branch with a 254 μm port pitch followed by two Y-branches with 127 μm pitch. Such a cascade arrangement allows the splitting of one input optical signal into four output optical signals. This approach is used for design and optimization of further split ratios 1 × 8, 1 × 16, 1 × 32, 1 × 64, and even more complex splitting structures, like 1 × 128 Y-branch optical splitters.

All Y-branch splitters were simulated at telecommunication operating wavelength, λ = 1.55 μm for transverse electric (TE), and transverse magnetic (TM) polarization and the starting field was set as a modal waveguide mode. The simulation results were almost identical for both polarizations. Since the TE polarization features lower losses, these simulation results are presented in this paper. Fig. 6 shows the simulation results of 1 × 128 Y-branch splitter structure with different S-Bend waveguide shapes (Arc, Cosine, Sine) and waveguide core size (6 × 6) μm^2. The field distribution at the end of simulated structure together with a background crosstalk (BX) is shown in Figs. 6(a), 6(c), 6(e). As can be seen, applying different S-Bend waveguide shapes has nearly no influence on this performance parameter. Detailed view of the field distribution showing the non-uniformity (ILu) and the insertion loss (IL) is presented in Figs. 6(b), 6(d), 6(f). From the simulations is evident that the insertion loss improved with the use of Cosine and Sine S-Bend waveguide shapes. The same applies to non-uniformity parameter.

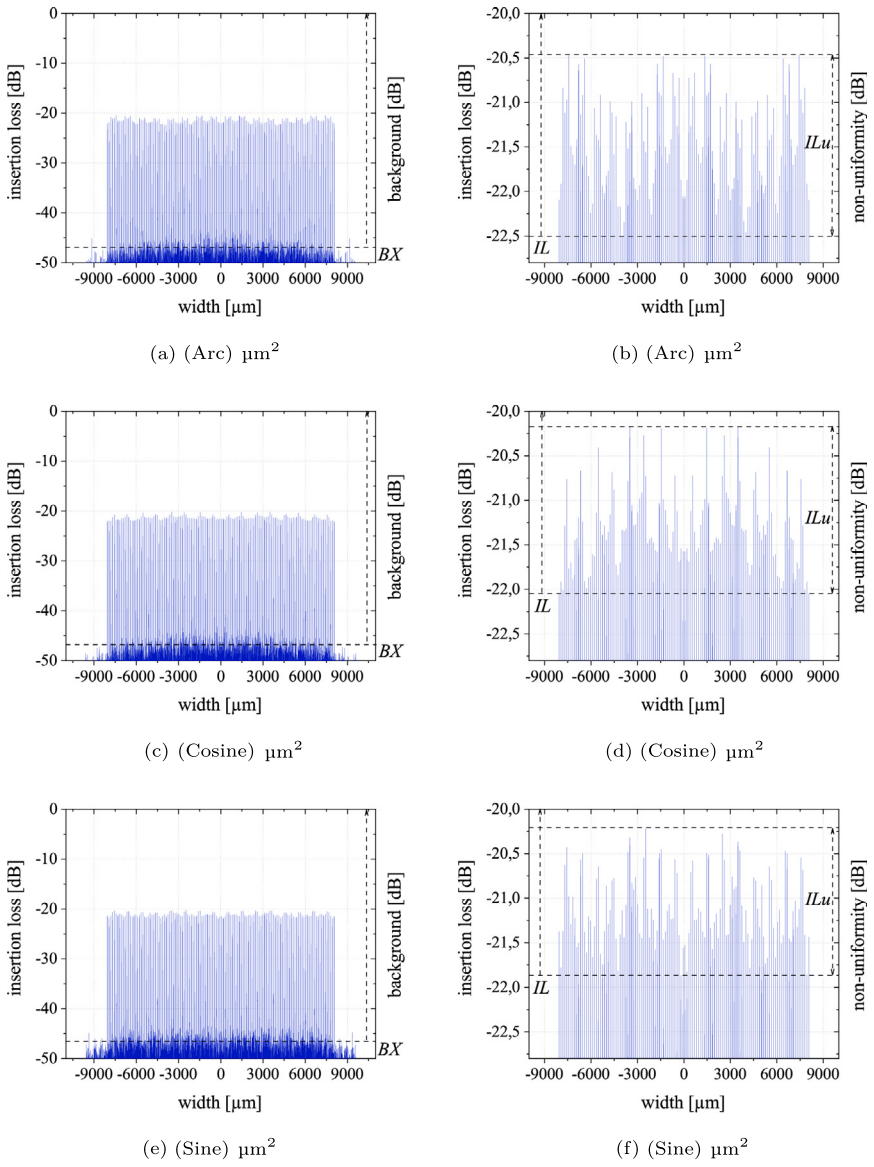

Fig. 6. Simulation results of 1 × 128 Y-branch splitter with different S-Bend shapes and waveguide core size (6 × 6) µm², (a) (c) (e) field distribution at the end of simulated structure together with a background crosstalk (BX), (b) (d) (f) detailed view of field distribution showing the non-uniformity (ILu) and the insertion loss (IL).

3.3. Core size optimization

The light can propagate in the waveguides in different modes. The number of propagating modes depends on the waveguide core dimensions, material, and the refractive index difference between core and cladding. How strongly the optical power is confined to the waveguide core depends on each mode. A mode is characterized by an invariant transversal intensity profile and an effective refractive index n_{eff}. When the effective index is higher than the cladding index, the modes are called guided, or fundamental modes [37]. The fundamental modes normally evince rather small propagation losses. Their field distribution declines exponentially in the cladding ensuring that the light beam is restricted to propagate in the core and intermediate vicinity. When the light beam is guided to the center of the core, one may inject some part of the power into cladding modes, if the input light is not well adjusted to the guided mode. Their intensity distribution fills the full cladding region, so they have often large power losses [38].

Fig. 7(c) shows that there is only one intensity maximum in the fundamental mode, i.e., the beam is straight and centered in the middle of the waveguide so that the light can be split evenly into the branches. The first mode contains a maximum and a minimum (see Fig. 7(d)). Thus, the beam is attenuated and is not guided to the center of the waveguide. From this follow, the best splitting results can be achieved by selecting a waveguide core size that supports only the fundamental mode [39].

In the case of (6 × 6) µm² waveguide core size, which was used in the splitter design, there are two existing propagating modes: TE0 mode with n_{eff} = 1.451 and TE1 mode with n_{eff} = 1.445, see Fig. 7. The fundamental mode, also called zero mode (TE0) is categorized as a guided mode since 1.451 > 1.445, and because the first mode (TE1) has the same refractive index value as a cladding, it is categorized as a cladding mode.

To see the influence of the waveguide core size on the Y-branch splitting ratio the waveguide core size was reduced from (6 × 6) µm² to (5.5×5.5) µm² and (5 × 5) µm² to boost only the fundamental mode light propagation. In the waveguide having the core size (5.5×5.5) µm² only one mode with the n_{eff} = 1.450 was calculated and the waveguide having core size (5 × 5) µm² has also one mode with n_{eff} = 1.449. Both modes belong to the guided modes because their effective index is higher than the refractive index of the cladding.

The same approach of length optimization, as described in Section 3.1, was applied to all splitters with the waveguide core size of

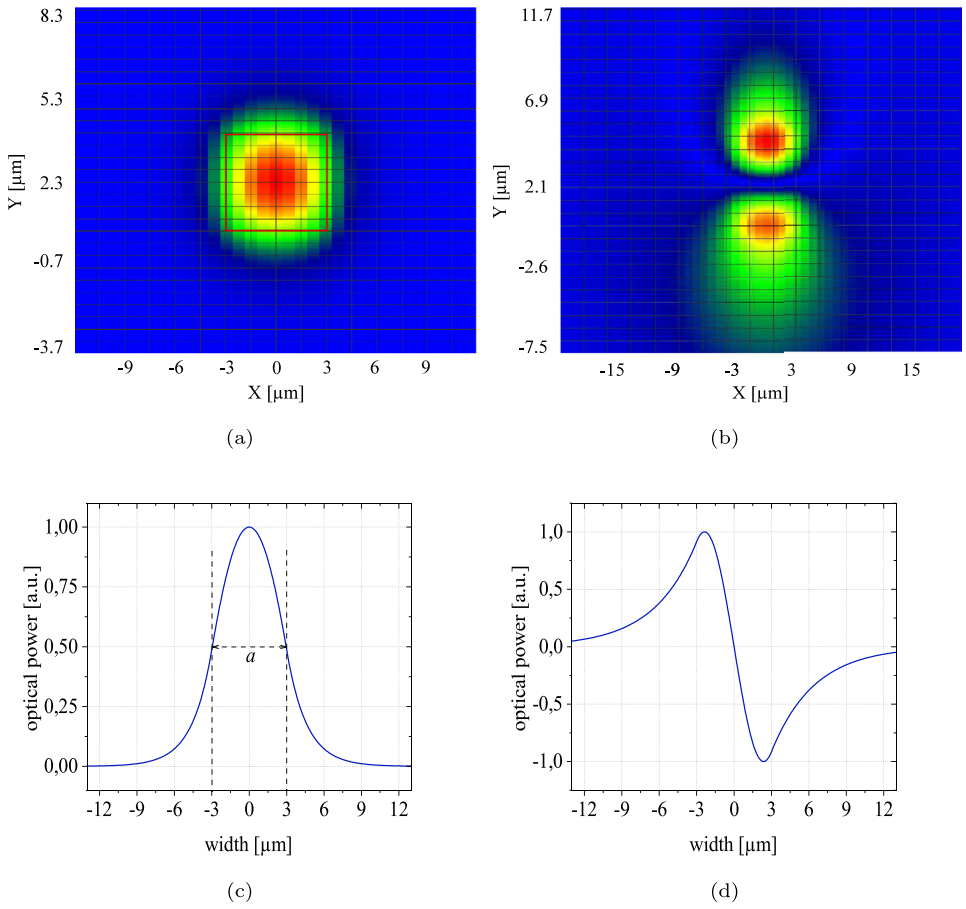

Fig. 7. Optical field in the (6 × 6) µm^2 waveguide: (a) TE0 mode, (b) TE1 mode. Field amplitude profiles: (c) TE0 mode, *a* represents the width of the waveguide, (d) TE1 mode.

Table 2
Summary of lengths of Y-branches in the 1 × 128 splitter with different waveguide shapes for waveguide core size (5.5 × 5.5) µm^2 and (5 × 5) µm^2.

Length of Y-branch [µm]	Core size [µm^2]					
	(5.5 × 5.5) Waveguide shape			(5 × 5) Waveguide shape		
	Arc	Cosine	Sine	Arc	Cosine	Sine
L(1st)	43000	17500	22500	38000	16000	21000
L(2nd)	28000	16000	14000	18000	12500	13500
L(3rd)	22000	13500	13500	16000	11000	11500
L(4th)	15000	10500	12000	11500	9500	6000
L(5th)	10000	8500	7000	8500	8000	3500
L(6th)	5000	5500	4000	4000	4000	2500
L(7th)	2600	2300	1700	2100	2000	1400

(5.5 × 5.5) µm^2 and of (5 × 5) µm^2. Table 2 shows the lengths of particular branches with the waveguide core size of (5.5 × 5.5) µm^2 and of (5 × 5) µm^2. The port pitches between the branches remained the same in all splitters as in the case of splitters with a waveguide core size of (6 × 6) µm^2.

Fig. 8 shows the graphical representation of the performance of the waveguide core-optimized 1 × 128 Y-branch splitters with S-Bend Arc shape, i.e., the field distribution achieved at the end of the simulation together with parameter BX. The simulations show that reducing the size of the waveguide core, BX increased. On the other hand, the insertion loss decreased. Nerveless, the highest improvement was achieved for non-uniformity parameter ILu.

4. Mathematical analysis

Design and simulation of passive optical components are performed by a commercial photonic tool BeamPROP from Optiwave. This tool uses BPM method based on the parabolic or paraxial approximation of the Helmholtz equations. Such a model then simplifies the simulations, reduces the processing time, and better manages the computer memory. Two-dimensional BPM isotropic simulation was performed for every 1×2^N Y-branch splitter. The 2D BPM simulator is based on the finite difference method algorithm of Crank–Nicolson [40]. For the simulation, the perfectly matched layer (PML) boundary condition is selected. It defines the truncation of the computation domain by layers without any reflection, irrespective of their frequency and angle of incidence [41].

Telcordia GR1209 & GR-1221 standards outline the generic criteria for the passive optical components to determine the quality of the PLC splitters over their product lifecycle. The standards specify general requirements for an outside plant component, the functional criteria, and the performance criteria [42].

For simulation purposes to evaluate the optical performance of the proposed splitters, the criteria as non-uniformity, insertion loss, and background crosstalk are essential, and therefore they were calculated. For symmetrical Y-branches, the optical power at each output port is approximately half of the optical power from the input port. The output signals have theoretically an equal amplitude, 0° phase relationship between any two output signals, and high isolation between each output signal [43]. The theoretical insertion loss [44] is defined mathematically as:

$$L(dB) = 10log_{10}(N) \quad (1)$$

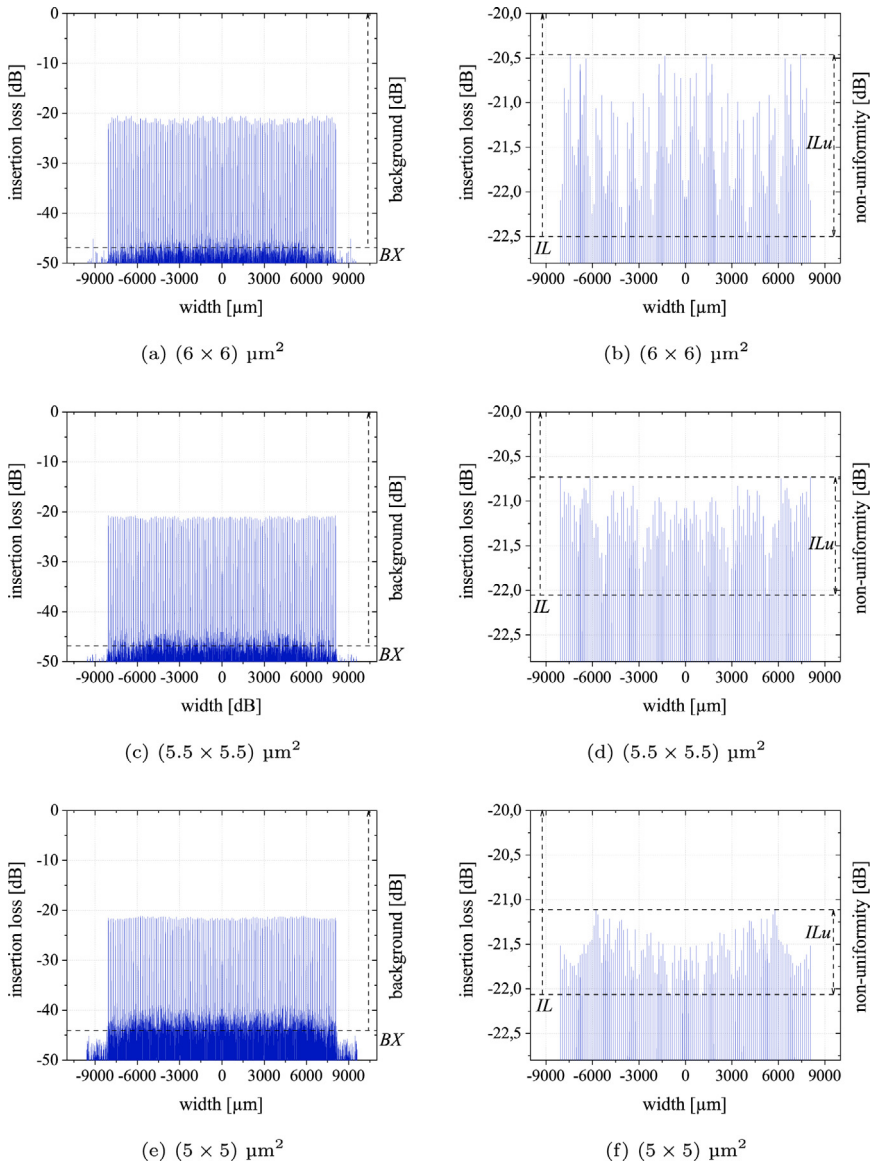

Fig. 8. Simulation results of 1 × 128 Y-branch splitter with S-Bend Arc shape and different waveguide core sizes: (6 × 6) µm², (5.5 × 5.5) µm², (5 × 5) µm²: (a) (c) (e) field distribution at the end of simulated structure together with a background crosstalk (BX), (b) (d) (f) detailed view of field distribution showing the non-uniformity (ILu) and the insertion loss (IL).

where $L(dB)$ is the insertion loss in decibels, and N is the number of output ports. For instance, in the case of a simple 1 × 2 Y-branch splitter, the theoretical insertion loss is $10log_{10}(2) = 3$ dB.

Insertion loss. The fraction of power transferred from the input port to the output port, i.e., insertion loss (IL) [45] is calculated after simulation for each port separately by:

$$IL(dB) = -10log_{10}\left[\sum_{i=1}^{N}\frac{I_i}{I_{in}}\right] \tag{2}$$

where I_i is the output energy from the i^{th} output waveguide, and I_{in} is the energy in the input waveguide. The maximum insertion loss is taken as a final insertion loss of the whole designed splitter.

Non-uniformity. Another parameter which was calculated is insertion loss uniformity (ILu, also called non-uniformity) [46], which is the difference between the maximum insertion loss (I_i) and minimum insertion loss (I_i) of the optical signal in the characteristics:

$$ILu(dB) = -10log_{10}\left[\frac{min_{(I_i)}}{max_{(I_i)}}\right] \tag{3}$$

Background crosstalk. Background crosstalk calculation (BX) does not exist in the standard formula yet. For this calculation, the point of the highest saturation (S_i) and the highest background crosstalk (B_i) value is taken into consideration. The final background value is the median transmission value from these two values.

$$BX(dB) = \frac{max_{(S_i)} + max_{(B_i)}}{2} \tag{4}$$

5. Results and discussion

In the first phase of the paper, the length for every pre-defined waveguide shape available in the OptiBPM tool was optimized. Fig. 9 shows the relations between the optical properties of 1×2^N Y-branch splitters ($N = 2, \ldots, 128$) and increasing number of outputs for a waveguide core size of (6 × 6) µm².

Fig. 9(a) shows the non-uniformity dependence on the number of output ports for all simulated shapes, Arc, Cosine, and Sine. As can be seen, the sinusoidal shape ensures the lowest non-uniformity for splitters with a higher number of outputs (32, 64, 128).

In the case of insertion losses, see Fig. 9(b), the Sine and Cosine S-Bend waveguide shapes are the most approached to theoretical values

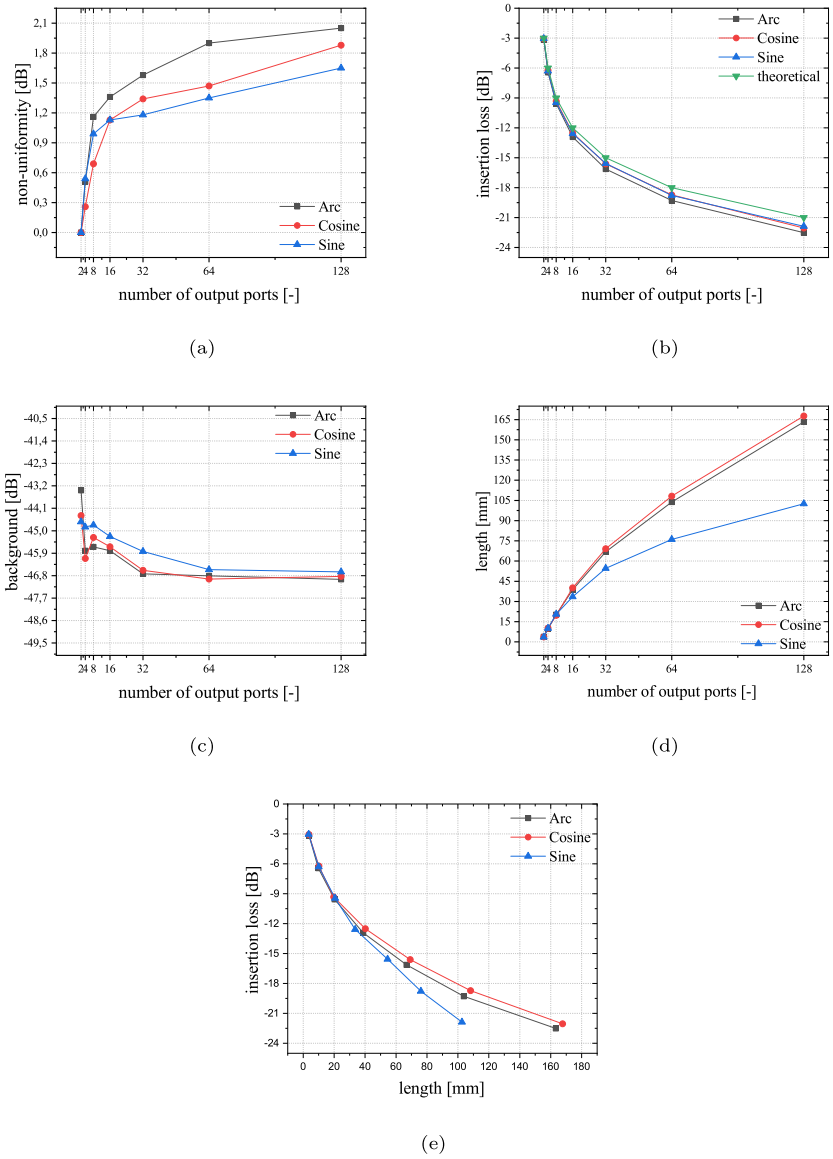

Fig. 9. Comparison of 1 × 2 to 1 × 128 Y-branch splitter performance parameters: (a) non-uniformity dependency on increasing number of output ports, (b) comparison of simulated and theoretical insertion loss on increasing number of output ports, (c) background dependency on increasing number of output ports, (d) length dependency of Y-branch splitters on increasing number of output ports, (e) insertion loss dependency on the length of Y-branch splitters.

of insertion loss. For the Arc S-Bend shape, the deviation slightly increases with the higher numbers of outputs.

Fig. 9(c) shows the dependence of the background crosstalk parameter on increasing number of output ports for different S-Bend waveguide shapes. As can be seen, the Sine S-Bend shape ensures the best performance parameters such as insertion loss and non-uniformity, but on the other hand, it features the highest background crosstalk values. In the case of Cosine and Arc S-Bend shapes, the background crosstalk values are very similar to each other.

Optimizing all three S-Bend lengths, the Sine S-Bend waveguide shape offers a significantly shorter length of the resulting 1 × 128 splitters, see in Fig. 9(d)–Fig. 9(e). Although the 1 × 128 Y-branch splitter with Cosine S-bend waveguide shape has better optical properties than the splitter with Arc S-Bend shape, it is longer. In Fig. 9(d) can be seen that the length of individual Y-branch splitters increases almost linear each time the number of ports was doubled and the length of splitters with a Sine S-Bend shape increases exponentially.

The dependency of the insertion loss on the length of the optimized Y-branch splitters is shown in Fig. 9(e). This dependency is similar to dependency in Fig. 9(b). The insertion loss is increasing exponentially with the growing length of the Y-branch splitters as well as with the increasing number of the output ports because the length and number of output ports are dependent on each other. The 1 × 128 Y-branch splitter with a Sine S-Bend shape has reached again the shortest length. The 1 × 128 Y-branch splitter with a Cosine S-Bend shape was the longest but, in the end, it achieved better optical properties compared to splitter with an Arc S-Bend shape waveguides.

In the second phase, the size of the waveguide core was reduced to $(5.5 \times 5.5)\ \mu m^2$ and further to $(5 \times 5)\ \mu m^2$ to suppress the first mode of 1 × 128 Y-branch splitter. With each change of the waveguide core size, the 1 × 128 Y-branch splitters were re-optimized for length. The core resizing was applied to the splitters with all three S-Bend types: Arc, Cosine, and Sine. Fig. 10 shows the results of the optical properties of 1 × 128 Y-branch splitters for all S-Bend types along with the reduction of the waveguide core size.

Fig. 10(a) shows how the non-uniformity was improved for applied S-Bend shapes when the size of the waveguide core was reduced. As can be seen, the most noticeable improvement occurred in the case of Arc S-Bend shape, where the non-uniformity of 1 × 128 Y-branch splitter

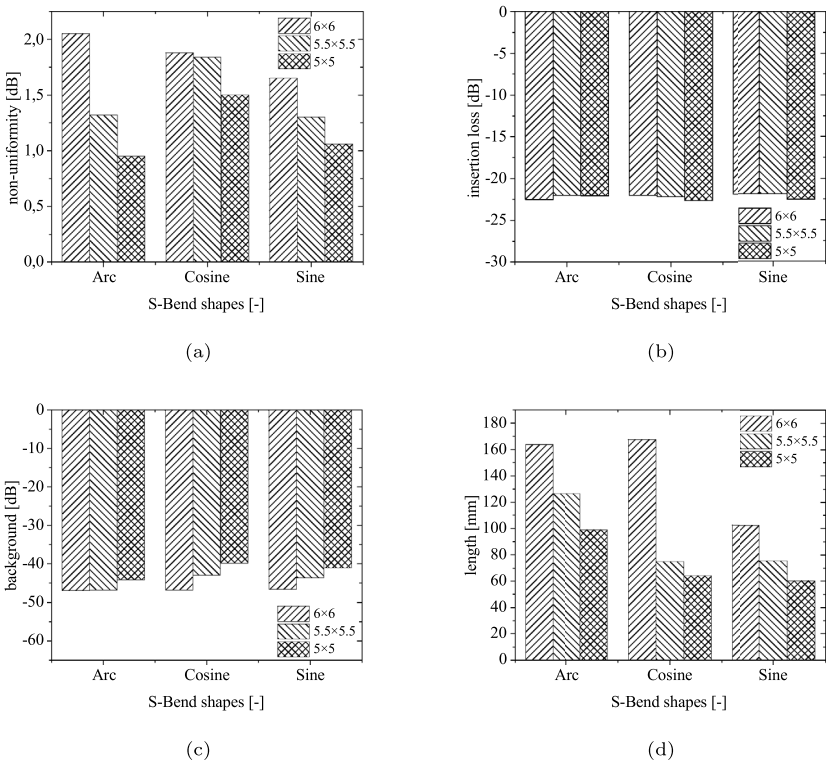

Fig. 10. Comparison of 1 × 128 Y-branch splitters parameters for different waveguide core sizes applied for different S-Bend shapes: (a) non-uniformity (ILu), (b) insertion losses (IL), (c) background crosstalk (BX), (d) length of the splitters.

was suppressed to more than half of its original value (from 2.05 dB to 0.95 dB).

Fig. 10(b) shows the calculated insertion loss at the end of the simulation. For all S-Bend waveguide shapes the insertion loss of the splitters did not improve significantly with the reduction of the waveguide core size. Therefore, the small diversity of final values of the insertion loss can be neglected.

Background crosstalk is shown in Fig. 10(c). This value is the only one that has worsened when optimizing the waveguide core size of the 1 × 128 Y-branch splitters. In the case of Arc S-Bend shape, it remained almost the same applying the core size (5.5×5.5) μm^2, and the background value with a core size (5 × 5) μm^2 deteriorated slightly. In the case of the Cosine and Sine S-Bend shapes, the background crosstalk values became worse with both reductions of the waveguide core size.

Significant improvement of the length of 1 × 128 Y-branch splitter by decreasing waveguide core size is shown in Fig. 10(d). In the case of Arc and Sine S-Bend shapes, the splitter length decreased linearly with decreasing waveguide core size (about one-third). In the case of Cosine S-Bend waveguide shape, the length of the splitter shortened dramatically to less than half when optimizing waveguide core size from (6 × 6) μm^2 to (5.5×5.5) μm^2. The further reduction did not have such a significant influence on the splitter length.

The numerical results of the 1 × 128 Y-branch splitter simulations for all S-Bend types together with the optimization of waveguide core size are shown in Table 3. If only the Y-branch splitter length optimization was considered (see column "chip size" in Table 3), the best results were achieved for the Y-branch splitter with a (5 × 5) μm^2 waveguide core size and Sine S-Bend shape, which reached 60400 μm. But if all optical properties of the splitters (see column "ILu", "IL" and "BX" in Table 3) were considered independent on the length, one of the best results was achieved for the Y-branch splitter having a (5 × 5) μm^2 waveguide core size and Arc S-Bend shape.

Table 3
Summary of the optical properties for 1 × 128 Y-branch splitters with Arc, Cosine, Sine S-Bend waveguide shapes and waveguide core sizes (6 × 6) μm^2, (5.5 × 5.5) μm^2, and (5 × 5) μm^2.

S-Bend shape	Core size [μm^2]	ILu [dB]	IL [dB]	BX [dB]	chip size [μm^2]
Arc	6 × 6	2.05	−22.51	−46.95	163800 × 16129
	5.5 × 5.5	1.31	−22.05	−46.79	126600 × 16129
	5 × 5	0.95	−22.06	−44.18	99100 × 16129
Cosine	6 × 6	1.88	−22.05	−46.83	167700 × 16129
	5.5 × 5.5	1.84	−22.17	−42.92	74800 × 16129
	5 × 5	1.50	−22.65	−39.84	64000 × 16129
Sine	6 × 6	1.65	−21.87	−46.65	102600 × 16129
	5.5 × 5.5	1.30	−21.86	−43.65	75700 × 16129
	5 × 5	1.06	−22.55	−41.11	60400 × 16129

6. Conclusion

In this paper, the Y-branch splitters up to 128 outputs with a silica-on-silicon material platform for telecommunication applications have been designed, simulated, and optimized. Detailed analyses of the impact of the S-Bend waveguide shapes were presented, with a particular focus on length optimization of the whole splitter structure. The results show that for a standard waveguide core size (6 × 6) μm^2, the shortest length was achieved for 1 × 128 Y-branch splitter with the Sine S-Bend waveguide shape, as shown in Table 3.

To reach further optimization, the core size of the waveguide was reduced to (5.5×5.5) μm^2 and (5 × 5) μm^2 to support only fundamental mode propagation. The results showed that the smaller waveguide core size ensures not only smaller footprint of the splitter but also satisfying optical performance.

Considering both, the size and performance optimization, the splitter with Sine S-Bend waveguide shape and waveguide core size (5.5 × 5.5) μm^2 had the best-achieved results. The splitter with Sine S-Bend waveguide shape was again leading in the case of waveguide core size (5 × 5) μm^2. The splitter with Arc S-Bend shape achieved better optical

properties but the length of the splitter was longer compared to the splitter with a Sine S-Bend waveguide shape.

Declaration of competing interest

The authors declare that they have no known competing financial interests or personal relationships that could have appeared to influence the work reported in this paper.

Acknowledgments

This work was supported by Campaign Slovakia-Austria (SAIA, n. o. and OeAD-GmbH) under project No. 2020-10-15-001 and Austrian Cooperative Research under project No. 521028.

References

[1] R. Matsumoto, T. Kodama, S. Shimizu, R. Nomura, K. Omichi, N. Wada, K.-I. Kitayama, 40G-OCDMA-PON system with an asymmetric structure using a single multi-port and sampled SSFB encoder/decoders, J. Lightwave Technol. 32 (6) (2014) 1132–1143.

[2] A. Usman, N. Zulkifli, M.R. Salim, K. Khairi, A.I. Azmi, Optical link monitoring in fibre-to-the-x passive optical network (FTTx PON): A comprehensive survey, Opt. Switch. Netw. (2020) 100596.

[3] B. Fröhlich, J.F. Dynes, M. Lucamarini, A.W. Sharpe, S.W.-B. Tam, Z. Yuan, A.J. Shields, Quantum secured gigabit optical access networks, Sci. Rep. 5 (1) (2015) 1–7.

[4] S. Bindhaiq, A.S.M. Supa, N. Zulkifli, A.B. Mohammad, R.Q. Shaddad, M.A. Elmagzoub, A. Faisal, et al., Recent development on time and wavelength-division multiplexed passive optical network (TWDM-PON) for next-generation passive optical network stage 2 (NG-PON2), Opt. Switch. Netw. 15 (2015) 53–66.

[5] K. Voigt, L. Zimmermann, G. Winzer, K. Petermann, C. Weinert, Silicon-on-insulator 90° optical hybrid using 4× 4 waveguide couplers with C-band operation, in: 2008 34th European Conference on Optical Communication, IEEE, 2008, pp. 1–2.

[6] Y. Shibata, N. Kikuchi, Y. Tohmori, Photonic integrated devices for high speed signal processing and switching, in: Optical Fiber Communication Conference, Optical Society of America, 2003, p. FF1.

[7] M.G. Kuzyk, C.W. Dirk, et al., Characterization Techniques and Tabulations for Organic Nonlinear Optical Materials, Marcel Dekker, 1998.

[8] G. Lifante, Integrated Photonics: Fundamentals, Wiley Online Library, 2003.

[9] L. Chrostowski, M. Hochberg, Silicon Photonics Design: From Devices To Systems, Cambridge University Press, 2015.

[10] L.B. Soldano, F.B. Veerman, M.K. Smit, B.H. Verbeek, A.H. Dubost, E.C. Pennings, Planar monomode optical couplers based on multimode interference effects, J. Lightwave Technol. 10 (12) (1992) 1843–1850.

[11] T. Rasmussen, J.K. Rasmussen, J.H. Povlsen, Design and performance evaluation of 1-by-64 multimode interference power splitter for optical communications, J. Lightwave Technol. 13 (10) (1995) 2069–2074.

[12] M. Bachmann, M. Smit, P. Besse, E. Cini, H. Melchior, L. Soldano, Polarization-insensitive low-voltage optical waveguide switch using InGaAsP/lnP four-port mach-zehnder interferometer, in: Optical Fiber Communication Conference, Optical Society of America, 1993, TuH3.

[13] S. Serecunova, D. Seyringer, F. Uherek, H. Seyriger, Comparison of optical properties of 1x128 splitters based on Y-branch and MMI approaches, in: Optical Components and Materials XVIII, Vol. 11682, International Society for Optics and Photonics, 2021, 116821N.

[14] W. Jiang, Highly uniform and polarization-independent Y-branch with mode filter based on deeply etched silica-on-silicon waveguide, Opt. Laser Technol. 111 (2019) 20–24.

[15] T. Hu, H. Qiu, Z. Zhang, X. Guo, C. Liu, M.S. Rouifed, C.G. Littlejohns, G.T. Reed, H. Wang, A compact ultrabroadband polarization beam splitter utilizing a hybrid plasmonic Y-branch, IEEE Photonics J. 8 (4) (2016) 1–9.

[16] O. Katz, D. Malka, Design of novel SOI 1× 4 optical power splitter using seven horizontally slotted waveguides, Photon. Nanostruct.: Fundam. Appl. 25 (2017) 9–13.

[17] D. Malka, Y. Sintov, Z. Zalevsky, Design of a 1× 4 silicon-alumina wavelength demultiplexer based on multimode interference in slot waveguide structures, J. Opt. 17 (12) (2015) 125702.

[18] D. Dai, H. Wu, Realization of a compact polarization splitter-rotator on silicon, Opt. Lett. 41 (10) (2016) 2346–2349.

[19] J.S. Yu, J.Y. Moon, S.M. Choi, Y.T. Lee, Fabrication of 1× 8 multimode-interference optical power splitter based on InP using CH4/H2 reactive ion etching, Japan. J. Appl. Phys. 40 (2R) (2001) 634.

[20] P. Gašo, D. Pudiš, D. Seyringer, A. Kuzma, L. Gajdošová, T. Mizera, M. Goraus, 3D polymer based 1 × 4 beam splitter, J. Lightwave Technol. 39 (1) (2020) 154–161.

[21] V. Prajzler, J. Zázvorka, Polymer large core optical splitter 1× 2 Y for high-temperature operation, Opt. Quantum Electron. 51 (7) (2019) 1–13.

[22] D. Seyringer, J. Chovan, L. Gajdosova, D. Figura, F. Uherek, Comparison of silicon nitride based 1× 8 Y-branch splitters applying different waveguide structures, in: 2019 21st International Conference on Transparent Optical Networks (ICTON), IEEE, 2019, pp. 1–4.

[23] D. Seyringer, Arrayed Waveguide Gratings, in: SPIE Spotlight, SPIE Press, 2016, https://books.google.at/books?id=ruo2ngAACAAJ.

[24] X.J. Leijtens, B. Kuhlow, M.K. Smit, Wavelength filters in fibre optics, in: Arrayed Waveguide Gratings, Vol. 123, 2006, pp. 125–187.

[25] G.T. Reed, A.P. Knights, Silicon Photonics: An Introduction, John Wiley & Sons, 2004.

[26] L. Pavesi, et al., Silicon Photonics, vol. 94, Springer Science & Business Media, 2004.

[27] A.P. Knights, P.E. Jessop, Silicon waveguides for integrated optics, in: Optical Waveguides, CRC press, 2018, pp. 231–270.

[28] K.K. Lee, D.R. Lim, H.-C. Luan, A. Agarwal, J. Foresi, L.C. Kimerling, Effect of size and roughness on light transmission in a Si/SiO_2 waveguide: Experiments and model, Appl. Phys. Lett. 77 (11) (2000) 1617–1619.

[29] D. Martens, A.Z. Subramanian, S. Pathak, M. Vanslembrouck, P. Bienstman, W. Bogaerts, R.G. Baets, Compact silicon nitride arrayed waveguide gratings for very near-infrared wavelengths, IEEE Photonics Technol. Lett. 27 (2) (2014) 137–140.

[30] H. Takahashi, Y. Ohmori, M. Kawachi, Design and fabrication of silica-based integrated-optic 1* 128 power splitter, Electron. Lett. 27 (23) (1991) 2131–2133.

[31] L. Wang, J. An, J. Zhang, Y. Wu, J. Li, H. Wang, Y. Wang, P. Pan, F. Zhong, Q. Zha, et al., Design and fabrication of optical power splitters with large port count, Chin. Opt. Lett. 12 (9) (2014) 092302.

[32] K. KwangOk, C. HwanSeok, Real-time demonstration of extended 10g-EPON capable of 128-way split on a 100 km distance using OEO-based PON extender, in: 2016 International Conference on Information and Communication Technology Convergence (ICTC), IEEE, 2016, pp. 930–932.

[33] C. Burtscher, D. Seyringer, F. Uherek, J. Chovan, A. Kuzma, Design of low loss 1× 64 Y-branch splitter having symmetric splitting ratio and small footprint, in: The Tenth International Conference on Advanced Semiconductor Devices and Microsystems, IEEE, 2014, pp. 1–4.

[34] C. Burtscher, D. Seyringer, A. Kuzma, M. Lucki, Modeling and optimization of 1× 32 Y-branch splitter for optical transmission systems, Opt. Quantum Electron. 49 (12) (2017) 396.

[35] R. Agalliu, C. Burtscher, M. Lucki, D. Seyringer, Optical splitter design for telecommunication access networks with triple-play services, J. Electr. Eng. 69 (1) (2018) 32–38.

[36] Optiwave, OptiBPM overview, 2020, Accessed: 2020-11-23, https://optiwave.com/optibpm-overview/.

[37] S.K. Selvaraja, P. Sethi, Review on optical waveguides, Emerg. Waveguide Technol. 95 (2018) 98.

[38] N.d. optical fiber technology, basics of fibers, 2020, pp. 6–7, Accessed: 2020-07-28, https://spie.org/samples/FG16.pdf.

[39] C. Burtscher, M. Lucki, D. Seyringer, Comparison of optical properties of 1× 8 splitters based on Y-branch and MMI approaches, Romanian Rep. Phys. 67 (4) (2015) 1578–1585.

[40] Optiwave, Introduction to optiBPM, 2020, Accessed: 2020-09-15, https://optiwave.com/optibpm-manuals/bpm-introduction-to-optibpm/.

[41] Optiwave, Perfectly matched layer (PML), 2020, Accessed: 2020-03-13, https://optiwave.com/optibpm-manuals/bpm-perfectly-matched-layer-pml.

[42] B. Lee, Benchmarking the Performance of Next Generation High Speed Access Networks, Senko Advanced Components, 2015, p. 6,10, Accessed: 2020-03-13, https://www.senko.com/literature/Optical%20Splitter%20Whitepaper_02.pdf.

[43] Understanding Power Splitters. Mini-Circuits AN10-006, Department of Electrical and Computer Engineering College of Engineering. UC Santa Barbara, 1999, p. 1, Accessed: 2020-03-13, https://web.ece.ucsb.edu/~long/ece145a/Lab2_145A/powersplitters.pdf.

[44] R. Hranac, Two-way Splitters: A Peek Under the Hood, Broadband Library, 2018, Accessed: 2020-03-14, https://broadbandlibrary.com/rf-signal-level-2/.

[45] V. Prajzler, N.K. Pham, J. Špirková, Design, fabrication and properties of the multimode polymer planar 1×2 Y optical splitter, Radioengineering 21 (4) (2012) 1206.

[46] Thorlabs, Fiber Coupler Tutorials, Thorlabs, 2020, Accessed: 2020-03-14, https://www.thorlabs.com/newgrouppage9.cfm?objectgroup_id=10758.